One-Dimensional "Spirals": Novel Asynchronous Chemical Wave Sources

J.-J. Perraud,[1] A. De Wit,[2] E. Dulos,[1] P. De Kepper,[1] G. Dewel,[2] and P. Borckmans[2]

[1]*Centre de Recherche Paul Pascal, Université de Bordeaux I, Avenue A. Schweitzer, 33600 Pessac, France*

[2]*Service de Chimie-Physique/Center for Nonlinear Phenomena and Complex Systems, CP231-Université Libre de Bruxelles, 1050 Bruxelles, Belgium*

(Received 30 November 1992)

We report the experimental observation of an endogeneous antisymmetric wave source in a quasi-one-dimensional chemical system. Substantiated by numerical simulations, a theoretical interpretation relying on the interaction between Turing and Hopf modes is proposed.

PACS numbers: 82.20.Mj, 05.70.Ln

The stationary periodic patterns proposed by Turing, in 1952 [1], as a basis for morphogenesis, have only recently been observed [2] in the monophasic isothermal chlorite-iodide-malonic acid (CIMA) reaction [3,4]. The formation of a reversible complex of reduced mobility between activator iodine species and the starch used as a color indicator, creates the difference between the effective diffusivities of the activator and the other unbound species, i.e., chlorite, on which the Turing structures rely for their existence [5]. Indeed, when complexation is progressively relaxed, the experiments show [6,7] that a transition from standing periodic structures to time dependent phenomena in the form of traveling waves may occur. In the transition region, among a wealth of other spatiotemporal behaviors, we report the observation of endogeneous 1D sources emitting waves asynchronously to the left and to the right. We bring proof that these peculiar sources correspond to a localized stationary Turing state embedded in an oscillating background. They are thus of a nature different from that of various sources that have recently been observed in hydrodynamical problems [8,9].

The observation of Turing structures in a nonbiological relatively simple redox reaction was made possible by the use of new continuously fed spatial gel reactors [10] that are a prerequisite for reaching the asymptotic states and for testing their stability at a controlled distance from thermodynamic equilibrium. The original work has sparked off subsequent experimental [6,7,11–13] and theoretical [14,15] studies devoted to the determination of the role played by the gel matrix and the starch, the uncovering of the different possible pattern modes, and the understanding of the role of the feeding concentration ramps.

Our reactor (Fig. 1) consists of a rectangular thin strip of agarose gel, loaded with starch, and fed along two opposite sides from well stirred tanks containing nonreacting subsets of the reagents of the CIMA reaction. Malonic acid is introduced only in tank A and chlorite only in tank B. Reagents diffuse into the gel where reaction processes take place. If no spatial symmetry breaking instability occurs, concentration profiles establish naturally into isoconcentration planes parallel to the feed surfaces. High iodide concentrations are typically found along tank A and a dark blue band due to the formation of a starch-iodine-iodide complex is formed. On the opposite side, iodide and iodine are rapidly oxidized to iodate and the gel remains clear. Beyond critical conditions, Turing structures appear that break this symmetry due to the feeding.

As predicted by the invoked complexation and immobilization mechanism [5], a transition between stationary periodic (Turing modes) and propagating wavelike (Hopf modes) patterns is experimentally observed by decreasing the starch concentration [6]. At very low concentration, only waves could be observed. The starch content is, however, not an easily tunable parameter since its modification requires the manufacturing of a different strip. Nevertheless, a similar transition occurs for a given low enough starch concentration, by increasing the concentration of malonic acid. The possibility of independently tuning two bifurcations by varying two independent parameters is suggestive of the neighborhood of a

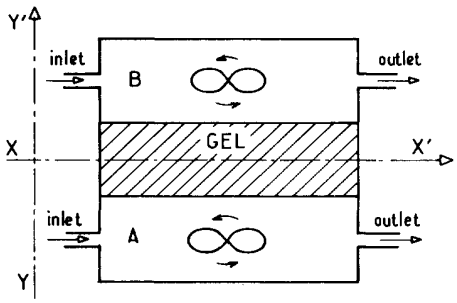

FIG. 1. In the reactor the gel strip is 10 mm long (XX' direction), 3 mm wide (YY' direction), and 0.14 mm thick. It is prepared by rapidly cooling a hot solution containing 0.9 g of Thiodène (a soluble starch from Prolabo) and 1 g of Agarose (Fluka 05070) in 50 ml of deionized water. It is then compressed between a white bottom plate and a transparent glass cover. Two opposite sides are in contact with the feeding tanks and the others with impermeable boundaries. $T=(2\pm0.5)°C$. The feed concentrations are (i) tank A $[KI]=2.5\times10^{-3}M$, $[CH_3CO_2H]=2.3M$, $[CH_2(CO_2H)_2]$ is the tunable parameter; (ii) tank B $[KI]=2.5\times10^{-3}M$, $[NaClO_2]=2.4\times10^{-2}M$, $[NaOH]=2.0\times10^{-2}M$.

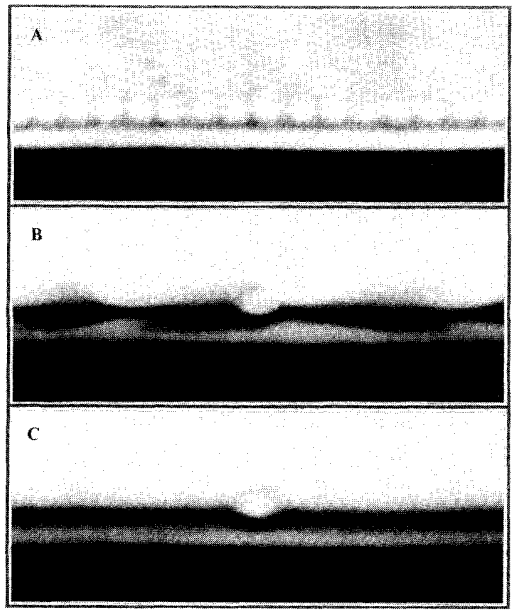

FIG. 2. (a) String of stationary Turing spots: Line of standing clear spots of oxidized state embedded in a band of the reduced darker state organized parallel to the feed boundaries (see Fig. 1); $[CH_2(CO_2H)_2]=0.5\times10^{-2}M$. (b) Antisymmetric pacemaker in a wave train state: Waves travel parallel to the feed boundaries with arrowhead shape. The clear edge of oxidation propagates into the darker recovery region with a rate of about 3 mm/min. The clear isolated Turing-like spot, near the middle of the figure, acts as an antisynchronous wave source. $[CH_2(CO_2H)_2]=1.0\times10^{-2}M$. (c) State averaged pattern obtained by averaging the dynamics of the wave train pattern (b) over several periods.

codimension 2 point.

Thus for a range of feed concentrations low in malonic acid, a Turing structure restricted to a narrow region can be obtained [Fig. 2(a)]: It forms a single line of clear spots, parallel to the feed boundaries, with a wavelength $\lambda=0.17\pm0.01$ mm. On comparing λ with the thickness of the gel strip (0.14 mm), one can infer that the pattern is effectively one dimensional. If the malonic acid concentration is then doubled, the bright spots die out while oscillatory behavior develops. After some time only wave trains remain, similar to those observed by Agladze, Dulos, and DeKepper [6], traveling parallel to the feed boundaries.

Very often, however, even after several hours, a few single bright spots (one to three) do not disappear and act as genuine 1D antisynchronous sources of wave trains [Fig. 2(b)]. The phenomenon is best represented by a space-time plot of the dynamics along a line parallel to the feed direction, passing through the source [Fig. 3(a)]. Clear bands of maximum intensity spread, alternatively to the right and to the left, with a time delay of 16 s, from a small region that essentially remains time invariant. The existence of a permanently brighter state at the wave source is clearly demonstrated in the time average picture [Fig. 2(c)]. Note that the size and relative intensity of the wave source region is similar to that of the individual spots making up the Turing pattern [Fig. 2(a)]. The source thus corresponds to a localized elementary Turing cell. Furthermore, the antiphase property of such a wave source does not result from a continuous spiraling wave in any plane since a time invariant region similar to that of Fig. 3(a) is found in the XX' direction at any vertical position in the YY' direction. The essence of the phenomenon is thus one dimensional [7].

Moreover, on further increasing malonic acid by 30%, all such sources disappear and waves propagate along the whole line. However, on resetting the control parameter to the lower value, isolated sources reappear after a few hours but generally at locations uncorrelated to the previous ones. They are thus truly endogeneous and not linked to defects or impurities trapped in the gel.

From the theoretical point of view, the existence in other fields of localized structures under uniform conditions has been shown in recent studies [16–19] to rely on two ingredients: multistability between various global states and dynamics not deriving from a potential function indicating the influence of so-called nonvariational effects [20,21]. These two elements are present in the vicinity of a Turing-Hopf codimension 2 bifurcation point where a pair of complex conjugate roots and a real root (with a wave number of the linear dispersion relation $|\underline{q}|=q_c\neq0$) simultaneously cross the imaginary axis on varying the bifurcation parameter.

If $\mathbf{C}$ is the vector of concentrations, $\mathbf{f}$ represents the reaction kinetics, and $\underline{D}$ is the diagonal matrix of positive diffusion coefficients, then near the Turing-Hopf point, the dynamics of a one-dimensional reaction-diffusion system

$$\frac{\partial \mathbf{C}}{\partial t}=\mathbf{f}(\mathbf{C})+\underline{D}\frac{\partial^2\mathbf{C}}{\partial x^2}$$

may be described by the superposition of Turing $T(X,\tau)$ and Hopf $H(X,\tau)$ fields:

$$\mathbf{C}(x,t)=\mathbf{C}_0+\mathbf{e}_T T(X,\tau)e^{iq_c x}+\mathbf{e}_H H(X,\tau)e^{i\Omega_c t}+\text{c.c.}$$

Here, $\mathbf{C}_0$ is the uniform reference state and $\mathbf{e}_T$ and $\mathbf{e}_H$ are respectively the critical Turing and Hopf eigenvectors of the linearized evolution operator. Ω_c is the linear frequency of the Hopf mode, i.e., the imaginary part of the complex root at the codimension 2 point.

The competition between such modes is then described by amplitude equations [22,23]. If X and τ are the slow space and time scales then

$$\frac{\partial T}{\partial \tau}=\mu_T T-g|T|^2T-\lambda|H|^2T+D^T\frac{\partial^2 T}{\partial X^2},$$

$$\frac{\partial H}{\partial \tau}=\mu_H H-(\beta_r+i\beta_i)|H|^2H-(\delta_r+i\delta_i)|T|^2H+(D_r^H+iD_i^H)\frac{\partial^2 H}{\partial X^2},$$

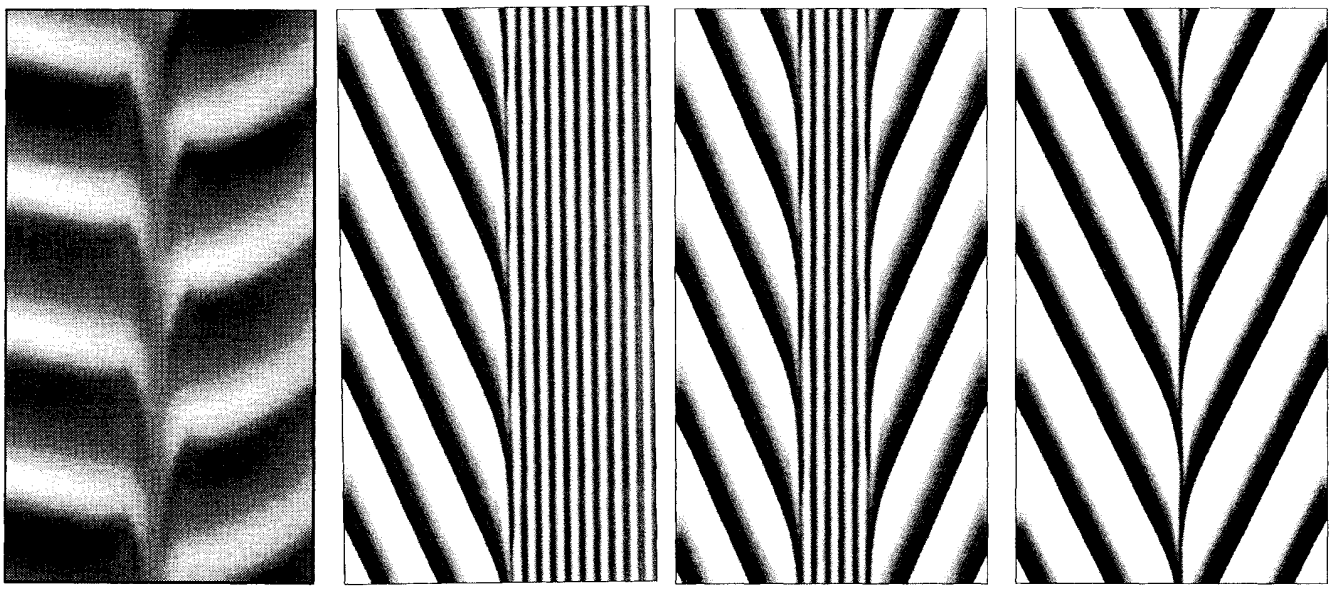

(a) (b) (c) (d)

FIG. 3. (a) Experimental space-time map [space: horizontal axis; time: vertical axis (running upwards)]. The light intensity along a line parallel to the feed boundaries, passing through the brightest part of the pacemaker, is plotted as a function of time. Bright lines correspond to clear wave fronts. The field view corresponds to 1.6 mm. The numerical space-time maps (b)–(d) are produced by integrating the reaction-diffusion equations of the 1D Brusselator model with an implicit integration scheme complemented with a finite difference method ($L=250$, $t=20$ adimensional units). No flux boundaries are assumed. The following values of the parameters are used: $A=2.5$, $D_X=4.11$, $D_Y=9.73$. Then both global Turing and Hopf modes are separately stable [24]. B is used as bifurcation parameter in this near codimension 2 situation. (b) Pinned front connecting a Turing pattern (right) to a train of plane waves (left) for $B=10.0$. (c) Droplet of a Turing structure embedded in a Hopf background emitting plane waves on both sides ($B=10.0$). (d) Endogeneous 1D spiral obtained by increasing in one step B to 12.5 starting from the front in (b). The waves are always emitted in phase opposition to the left and to the right. Multistability between such spirals, fronts, and localized Turing states is obtained for the same range of parameters. As an example, the localized structures (b) and (c) are still stable at $B=12.5$ if B is increased quasistatically in small steps.

where μ_T and μ_H are the two unfolding parameters. We assume in the following that D^T and D_r^H are positive and also g, β_r so that both bifurcations are supercritical. The above equations have in general a nonvariational structure. This dynamical system possesses three nontrivial global solutions: (i) a family of Turing structures

$$T=[(\mu_T-D^TQ^2)/g]^{1/2}e^{iQX},\quad H=0;$$

(ii) a one-parameter family of plane waves

$$T=0,\quad H=[(\mu_H-D_r^H\kappa^2)/\beta_r]^{1/2}e^{i(\Omega_\kappa\tau-\kappa X)}$$

with the frequency renormalization: $\Omega_\kappa=-\beta_i|H_\kappa|^2-D_i^H\kappa^2$, where H_κ is the preexponential factor in H; and (iii) a two-parameter family of mixed modes that we do not write down explicitly as we concentrate, among the many possible scenarios, on situations where the mixed modes are unstable and the system exhibits bistability between the pure global Turing and Hopf modes.

The ingredients to stabilize localized structures are therefore present. These may be formed by spatial juxtaposition of the global states as is corroborated by numerical simulations on the Brusselator [24], in the vicinity of such a codimension 2 point.

The simplest localized structure consists of a front [Fig. 3(b)] connecting a Turing pattern domain to a train of plane waves the wave vector and frequency of which are selected by the nonlinear dispersion relation. Since the width of the front is narrow, it may interfere with the underlying Turing structure leading to its pinning. As a result a stationary front is obtained for a finite range (locking band) of the bifurcation parameter values [25,26]. Beyond, but near the depinning transition, one observes, on the simulations, the characteristic oscillating velocity of the front. One wavelength to the Turing structure is added (subtracted) during every emitted wave period. The nonadiabatic effects responsible for this pinning escape standard amplitude equations analysis.

Those fronts may then serve as "building blocks" to construct droplets of one global state embedded into another [20,21,27–29]. Simulations have indeed produced such localized one-dimensional objects the core of which is formed by a Turing structure, truncated to a few wavelengths, emitting plane waves to both sides [Fig. 3(c)]. The amplitude of the plane waves goes to zero in

the core where conversely the Turing mode presents a local maximum but is absent elsewhere. We claim that the stability of such symbiotic Hopf hole and Turing pulse finds its origin in a combination of the pinning and nonvariational effects.

The number of wavelengths in the core and the phase relation between the waves emitted to the left and the right depend strongly on the initial conditions as intricate hysteresis effects are present. On varying the bifurcation parameter in the direction where the global Hopf mode becomes dominant, antisynchronous wave sources, analogous to the experimental ones, can readily be obtained [Fig. 3(d)]. They can be thought of as 1D spirals.

Simulations also produce the complementary localized structures where the Hopf mode is embedded in the Turing background. Such objects and localized Turing structures restricted to three wavelengths in the core have been observed transiently in experiments, suggesting a narrower range of stability or smaller basin of attraction.

These latter experimental observations, for parameters in the range for which the wave sources occur, comfort us in the belief that the competition between the Turing and Hopf modes is indeed important to explain the origin of all these localized sources.

We thank J. Boissonade, A. Arneodo, and D. Walgraef for stimulating discussions. P.B. and G.D. are Research Associates with the FNRS (Belgium) and A.D. is an IRSIA (Belgium) Fellow. This work was supported by the EC Science Program (Twinning No. SC1-CT91-0706). Centre de Recherche Paul Pascal is CNRS UP 78476.

[1] A. M. Turing, Philos. Trans. R. Soc. London, Ser. B **327**, 37 (1952).
[2] V. Castets, E. Dulos, J. Boissonade, and P. De Kepper, Phys. Rev. Lett. **64**, 2953 (1990).
[3] P. De Kepper, I. R. Epstein, K. Kustin, and M. Orban, J. Phys. Chem. **86**, 170 (1982).
[4] I. Lengyel, G. Rabai, and I. R. Epstein, J. Am. Chem. Soc. **112**, 4606 (1990); **112**, 9104 (1990).
[5] I. Lengyel and I. R. Epstein, Proc. Natl. Acad. Sci. USA **89**, 3977 (1992).
[6] K. Agladze, E. Dulos, and P. De Kepper, J. Phys. Chem. **96**, 2400 (1992).
[7] J.-J. Perraud, K. Agladze, E. Dulos, and P. De Kepper, Physica (Amsterdam) **188A**, 1 (1992).
[8] D. Bensimon, P. Kolodner, C. M Surko, H. Williams, and V. Croquette, J. Fluid Mech. **217**, 441 (1990).
[9] *Order and Turbulent Patterns in Taylor-Couette Flow,* edited by D. C. Andereck and F. Hayot (Plenum, New York, 1992).
[10] Z. Noszticzius, W. Horsthemke, W. D. McCormick, H. L. Swinney, and W. Y. Tam, Nature (London) **329**, 619 (1987).
[11] P. De Kepper, V. Castets, E. Dulos, and J. Boissonade, Physica (Amsterdam) **49D**, 161 (1991).
[12] Q. Ouyang and H. L. Swinney, Nature (London) **352**, 610 (1991).
[13] Q. Ouyang and H. L. Swinney, Chaos **1**, 411 (1991).
[14] P. Borckmans, A. De Wit, and G. Dewel, Physica (Amsterdam) **188A**, 137 (1992).
[15] V. Dufiet and J. Boissonade, J. Chem. Phys. **96**, 664 (1992).
[16] G. Ahlers, Physica (Amsterdam) **51D**, 421 (1991), and references therein.
[17] U. Middya, M. Sheintuch, M. D. Graham, and D. Luss, Physica (Amsterdam) **63D**, 393 (1993).
[18] H. Willebrand, T. Hünteler, F.-J. Niedernostheide, R. Dohmen, and H.-G. Pruwins, Phys. Rev. A **45**, 8766 (1992).
[19] H. H. Rotermund, S. Jakubith, A. von Oertzen, and G. Ertl, Phys. Rev. Lett. **66**, 3083 (1991).
[20] O. Thual and S. Fauve, J. Phys. (Paris) **49**, 182 (1988).
[21] W. van Saarloos and P. C. Hohenberg, Physica (Amsterdam) **D56**, 303 (1992).
[22] J. Guckenheimer and P. Holmes, *Nonlinear Oscillations, Dynamical Systems and Bifurcations of Vector Fields* (Springer, New York, 1983).
[23] H. Kidachi, Prog. Theor. Phys. **63**, 1152 (1980).
[24] G. Nicolis and I. Prigogine, *Self-Organization in Nonequilibrium Systems* (Wiley, New York, 1977).
[25] Y. Pomeau, Physica (Amsterdam) **23D**, 3 (1986).
[26] D. Bensimon, B. I. Shraiman, and V. Croquette, Phys. Rev. A **38**, 5461 (1988).
[27] S. Koga and Y. Kuramoto, Prog. Theor. Phys. **63**, 106 (1980).
[28] V. Hakim, P. Jakobsen, and Y. Pomeau, Europhys. Lett. **11**, 19 (1990).
[29] G. Dewel and P. Borckmans, Europhys. Lett. **17**, 523 (1992).

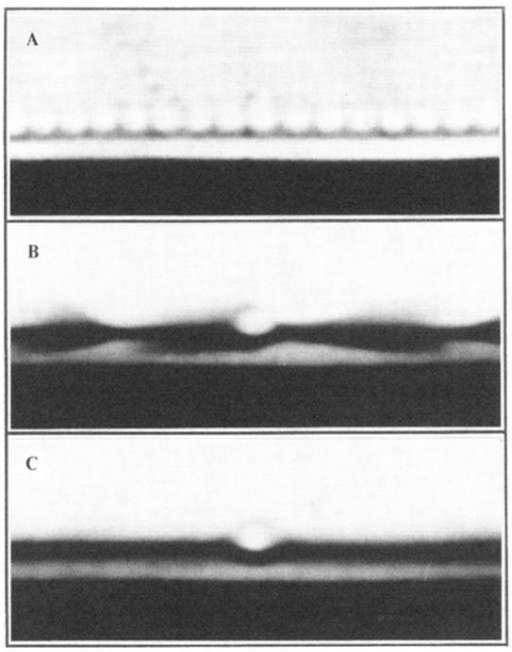

FIG. 2. (a) String of stationary Turing spots: Line of standing clear spots of oxidized state embedded in a band of the reduced darker state organized parallel to the feed boundaries (see Fig. 1); $[CH_2(CO_2H)_2] = 0.5 \times 10^{-2} M$. (b) Antisymmetric pacemaker in a wave train state: Waves travel parallel to the feed boundaries with arrowhead shape. The clear edge of oxidation propagates into the darker recovery region with a rate of about 3 mm/min. The clear isolated Turing-like spot, near the middle of the figure, acts as an antisynchronous wave source. $[CH_2(CO_2H)_2] = 1.0 \times 10^{-2} M$. (c) State averaged pattern obtained by averaging the dynamics of the wave train pattern (b) over several periods.

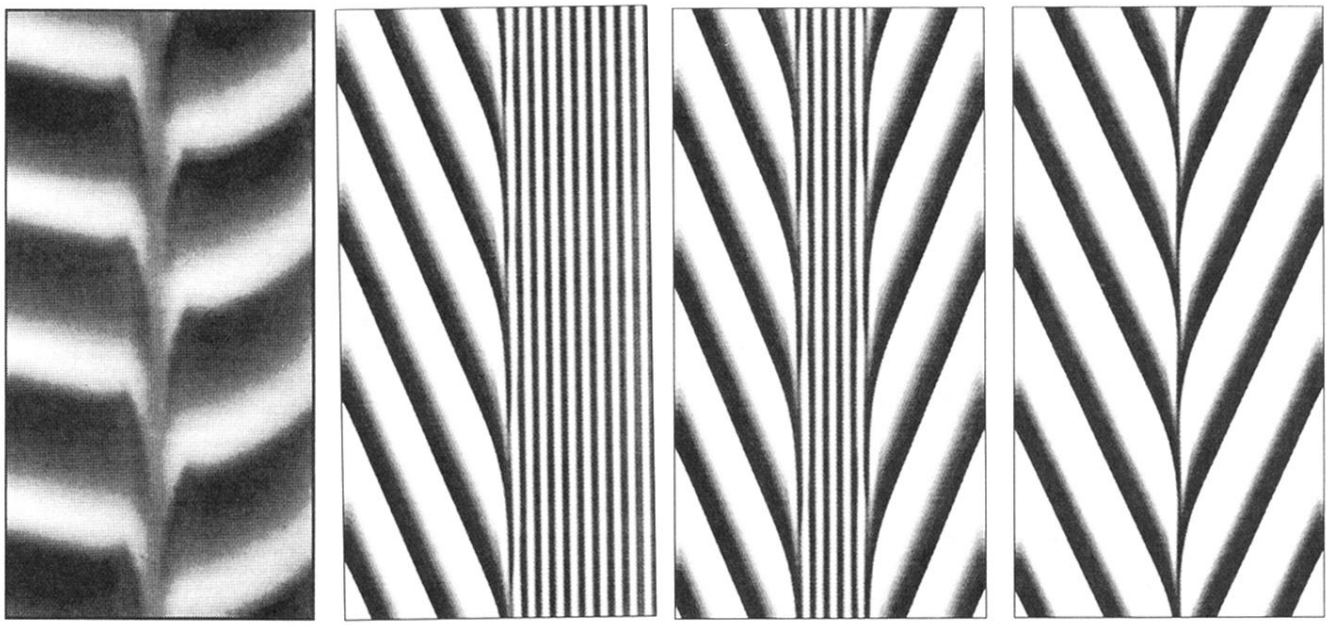

FIG. 3. (a) Experimental space-time map [space: horizontal axis; time: vertical axis (running upwards)]. The light intensity along a line parallel to the feed boundaries, passing through the brightest part of the pacemaker, is plotted as a function of time. Bright lines correspond to clear wave fronts. The field view corresponds to 1.6 mm. The numerical space-time maps (b)–(d) are produced by integrating the reaction-diffusion equations of the 1D Brusselator model with an implicit integration scheme complemented with a finite difference method ($L=250$, $t=20$ adimensional units). No flux boundaries are assumed. The following values of the parameters are used: $A=2.5$, $D_X=4.11$, $D_Y=9.73$. Then both global Turing and Hopf modes are separately stable [24]. B is used as bifurcation parameter in this near codimension 2 situation. (b) Pinned front connecting a Turing pattern (right) to a train of plane waves (left) for $B=10.0$. (c) Droplet of a Turing structure embedded in a Hopf background emitting plane waves on both sides ($B=10.0$). (d) Endogeneous 1D spiral obtained by increasing in one step B to 12.5 starting from the front in (b). The waves are always emitted in phase opposition to the left and to the right. Multistability between such spirals, fronts, and localized Turing states is obtained for the same range of parameters. As an example, the localized structures (b) and (c) are still stable at $B=12.5$ if B is increased quasistatically in small steps.